

# Experimental assessment of physical realism in a quantum controlled device

P. R. Dieguez<sup>1</sup>, J. R. Guimarães<sup>1</sup>, J. P. S. Peterson<sup>2</sup>, R. M. Angelo<sup>3</sup> and R. M. Serra<sup>1</sup>

<sup>1</sup>Center for Natural and Human Sciences, Federal University of ABC,  
Avenida dos Estados 5001, 09210-580, Santo André, São Paulo, Brazil

<sup>2</sup>Institute for Quantum Computing and Department of Physics and Astronomy,  
University of Waterloo, 200 University Avenue West, N2L 3G1, Waterloo, Ontario, Canada

<sup>3</sup>Department of Physics, Federal University of Paraná,  
PO BOX 19044, 81531-980, Curitiba, Paraná, Brazil

The quantum version of Wheeler’s delayed-choice experiment challenges interpretations of the complementarity principle based on post-quantum variables. With basis on the visibility at the output of a quantum controlled interferometer, a conceptual framework has been put forward which detaches the notions of wave and particle from the quantum state and allows for the existence of hybrid wave-particle behaviours, thus claiming for a critical review of the complementarity principle. Here, we propose and implement a contrast experimental setup which, upon analysis of an operational criterion of physical reality, proves to yield a dramatically different state of affairs. We show that, in disparity with previous proposals, our setup ensures a formal link between the visibility and elements of reality within the interferometer and predicts the existence of hybrid elements of reality interpolating between wave and particle. An experimental *proof-of-principle* is provided for a two-spin-1/2 system in an interferometric setup implemented in a nuclear magnetic resonance platform. Furthermore, our results validate, to a great extent, Bohr’s original formulation of the complementarity principle.

Although lacking an indisputable formulation in terms of the mathematical structure of quantum mechanics, Bohr’s complementarity principle [1] manifested its pivotal role in modern physics by submitting matter and radiation to an unifying framework: any one of these elements is expected to exclusively behave either in a *wave-* or in a *particle-like* manner, depending on the peculiarities of the experimental setup. Bohr’s natural philosophy [2] also advocates the impossibility of ascribing individuality to quantum systems, meaning that the physical reality cannot emerge until the whole experiment, including the system and the classical measuring apparatus, is definitely arranged. These ideas prompted Wheeler to devise the concept of a delayed-choice experiment [3], a scenario wherein the classical apparatus, typically an interferometer, is settled only when the quantum system has entered it. When this experiment came into actual existence [4–6], the observed visibility at the output of the interferometer always revealed the fingerprints of wave or particle in full agreement with the results expected for the (posteriorly defined) corresponding setting. The complementarity principle was not cheated by the delayed arrangement of “the whole”. Moreover, generalizations of Wheeler’s idea in terms of entanglement-separability duality of bipartite systems were also proposed [7–9] and experimentally confirmed in the context of delayed-choice entanglement swapping experiments [10, 11].

Nearly one decade ago, a quantum delayed-choice experiment (QDCE) was conceived [12] in which one beam-splitter is prepared in a spatial quantum superposition, thus rendering the interferometer to have a “closed + open” configuration and the system to be in a hybrid “wave + particle” state. To test these ideas, researchers

coupled a target system to a *quantum controller*—an ancilla in superposition that effectively implements a suspended configuration for the interferometer [13–16]. Besides allowing for the control of the superposition degree of the whole system, such strategy enables one to decide (measure) the configuration after the target has traversed the interferometer. The capability of such scheme to smoothly interpolate the observed statistics between a wave- and a particle-like pattern suggested the manifestation of “morphing behaviours” in the same setup, thus claiming for a radical revision of Bohr’s original statement of the complementarity principle [17]. More recently, variants of this experiment have reported on the observation of an entangled duality in a two-photon system [18], a which-path detector that can simultaneously record and neglect the system’s path information [19], and the implementation of a nonlocal setting control [20]. Entropic frameworks have offered alternative interpretations for the QDCE [21, 22] and the equivalence of such setting with a prepare-and-measure scenario in the perspective of device independent causal models has been demonstrated [23].

A common feature of all these experiments is the use of retro-inference about the system behaviour inside the interferometer with basis on the visibility observed at the output of the interferometer. To date, a detailed analysis is lacking which would allow one to track the behavior of the system at every stage of the experiment. Moreover, it is still not clear how elements of reality emerge from “the whole” and whether quantum correlations play some fundamental role. In this work, these questions are thoroughly addressed. First, we adopt an operational quantifier of realism that explicitly depends on the quantum state and allows for meaningful which-

path statements. This enables us to discuss realism for “the whole” by looking at the global state of the system at each instant of time. Second, we show that the visibility at the output has no connection whatsoever with wave and particle elements of reality, as defined in accordance with the adopted criterion of realism. This raises important objections to the usual interpretations of the QDCE. Third, we propose a setup that removes these objections and establishes a monotonic link between the visibility and wave elements of reality inside the interferometer. We then demonstrate the relevance of quantum correlations to wave-particle duality. Fourth, by use of a nuclear magnetic resonance (NMR) platform, we submit our model to experimental scrutiny. Finally, we argue how our results retrieve Bohr’s original view of the complementarity principle.

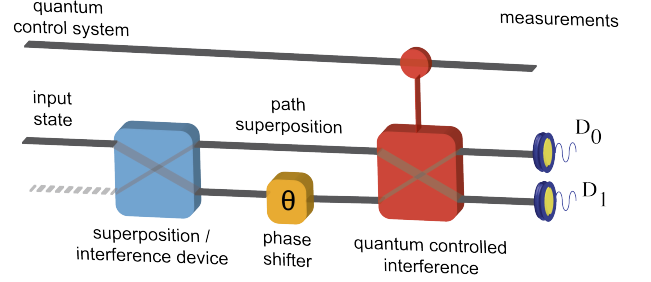
*Contextual realism in the QDCE.* Recently, a criterion of realism has been put forward [24] with basis on a single premise, namely, that after a projective measurement is performed of a physical quantity  $\mathcal{A}$ , represented by a discrete-spectrum observable  $A = \sum_a a A_a$ , with projectors  $A_a = |a\rangle\langle a|$  acting on  $\mathcal{H}_A$ , for a given preparation  $\varrho$  on  $\mathcal{H}_A \otimes \mathcal{H}_B$ , then  $\mathcal{A}$  becomes an element of reality, even if the measurement outcome is not revealed. Accordingly, the post-measurement state  $\Phi_A(\varrho) := \sum_a (A_a \otimes \mathbb{1}) \varrho (A_a \otimes \mathbb{1})$  is taken as a primitive notion of  $A$ -reality state. It then follows that

$$\mathcal{I}_A(\rho) := \min_{\varrho} S(\rho \| \Phi_A(\varrho)) = S(\Phi_A(\rho)) - S(\rho) \quad (1)$$

is a faithful quantifier of  $A$ -realism violations for a given state  $\rho$  (where  $S(\rho) := \text{Tr}(\rho \log_2 \rho)$  is the von Neumann entropy). By virtue of the properties of the relative entropy of  $\rho$  and  $\sigma$ ,  $S(\rho \| \sigma) = \text{Tr}[\rho(\log_2 \rho - \log_2 \sigma)]$ , the so-called *irrealism* of the context  $\{A, \rho\}$  is bounded as  $0 \leq \mathcal{I}_A(\rho) \leq \log_2 d_A$ , with  $d_A = \dim \mathcal{H}_A$ , vanishing iff  $\rho = \Phi_A(\rho)$ . This measure has been applied to a number of foundational investigations [25–32], including an experimental test in a photonic platform [33]. Also, irrealism has formally been framed as a quantum resource [34]. Two properties of irrealism will be crucial here. First, since  $\mathcal{I}_A(\rho) - \mathcal{I}_A(\rho_A) \geq \mathcal{D}_A(\rho)$  [24], where  $\rho_A = \text{Tr}_B(\rho)$  is the reduced state,  $\mathcal{D}_A(\rho) = \min_A [I_{A:B}(\rho) - I_{A:B}(\Phi_A(\rho))]$  is the quantum discord [35–38], and  $I_{A:B}(\rho) = S(\rho \| \rho_A \otimes \rho_B)$  denotes the mutual information, one has that, whenever quantum discord is present, the  $A$ -irrealism induced by the joint state  $\rho$  is greater than the one deriving from the part  $A$  alone. This shows that quantum correlations render irrealism to be a property of “the whole”. Second, the relation  $\mathcal{I}_A(\rho) + \mathcal{I}_{A'}(\rho) \geq S\left(\rho \| \frac{\mathbb{1}}{d_A} \otimes \rho_B\right)$  [39] concerning maximally incompatible observables  $A$  and  $A'$  acting on  $\mathcal{H}_A$  precludes the manifestation of full realism whenever  $\rho \neq \frac{\mathbb{1}}{d_A} \otimes \rho_B$ . For convenience, here we follow the ideas discussed in Ref. [25] to work instead with the  $A$ -realism

$$\mathfrak{R}_A(\rho) := \log_2 d_A - \mathcal{I}_A(\rho), \quad (2)$$

**a** Quantum controlled delayed choice scenario



**b** Quantum controlled reality scenario

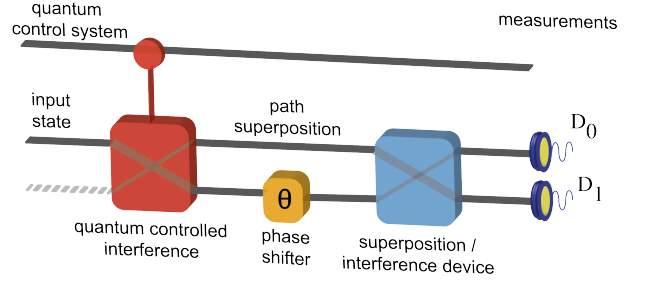


FIG. 1. Schematic circuits of quantum controlled interferometers. The blue boxes represent unitary operations which here play the role of superposition devices—the quantum network equivalent of a beam-splitter. Using an ancillary qubit in superposition (quantum control system), we implement the quantumly controlled unitary superposition device (represented by the red boxes). (a) Original version of the QDCE, where the second beam-splitter is prepared in a coherent superposition of being *in* and *out* of the interferometer (configurations *closed* and *open*, respectively). (b) Our proposal for the QDCE. Here, the first beam-splitter is submitted to quantum control. Although the measurement outcomes yield the same visibility in both of these experimental arrangements, the realism aspects inside the interferometer are crucially different.

which quantifies how close the scenario is to the  $A$ -realistic context  $\{\Phi_A(\rho), A\}$ . It follows from the above relations that  $\mathfrak{R}_A(\rho_A) - \mathfrak{R}_A(\rho) \geq \mathcal{D}_A$  (non-separability of  $A$ -realism) and

$$\mathfrak{R}_A(\rho) + \mathfrak{R}_{A'}(\rho) \leq \log_2 d_A + S(\rho_A) - I_{A:B}(\rho). \quad (3)$$

Notably, these correlations further restricts quantum systems to reach full realism. For pure states  $\rho = |\psi\rangle\langle\psi|$ , the upper bound becomes  $\log_2 d_A - E(\psi)$ , with  $E(\psi) = S(\rho_{A(B)})$  the entanglement entropy of  $|\psi\rangle$ .

Equipped with the above tools, we now reassess the QDCE (depicted in the first circuit in Fig. 1(a) from the perspective of elements of reality. As discussed in the original formulations [12], a qubit is put in a *particle-like state*  $|\varphi_\theta\rangle = \frac{1}{\sqrt{2}}(|0\rangle + e^{i\theta}|1\rangle)$  after passing the superposition device and the phase shifter, where  $\{0, 1\}$  denote the paths travelled by the qubit. On the other hand, when the final superposition device is activated (interferometer closed), then the state  $|\varphi_\theta\rangle$  transforms into the so-called

wave-like state  $|w_\theta\rangle = e^{i\theta/2}(\cos\frac{\theta}{2}|0\rangle - i\sin\frac{\theta}{2}|1\rangle)$ , with amplitudes clearly depending on the phase. By preparing the quantum controller ( $\mathcal{C}$ ) in a general coherent superposition  $\cos\frac{\alpha}{2}|\text{in}\rangle + \sin\frac{\alpha}{2}|\text{out}\rangle$ , the state at the output of the interferometer reads  $|\psi_{\mathbf{a}}\rangle = \cos\frac{\alpha}{2}|w_\theta\rangle|\text{in}\rangle + \sin\frac{\alpha}{2}|\varphi_\theta\rangle|\text{out}\rangle$ . The interference pattern in the detector  $D_0$  is then shown to be written as  $\mathbf{p}_0 = \text{Tr}(|0\rangle\langle 0| \otimes \mathbb{1}_{\mathcal{C}} \rho_{\mathbf{a}}) = \frac{1}{2}(1 + \mathcal{V}\cos\theta)$ , where  $\rho_{\mathbf{a}} = |\psi_{\mathbf{a}}\rangle\langle\psi_{\mathbf{a}}|$  and  $\mathcal{V} := (\mathbf{p}_0^{\max} - \mathbf{p}_0^{\min})/(\mathbf{p}_0^{\max} + \mathbf{p}_0^{\min}) = \cos^2(\frac{\alpha}{2})$ , which stands for the visibility of the interference pattern computed from optimizations running over  $\theta$ . The association of  $|w_\theta\rangle$  and  $|\varphi_\theta\rangle$  with wave- and particle-like behaviours is justified with basis on the resulting dependence of  $\mathbf{p}_0$  on the phase  $\theta$ , as can be readily checked for  $\alpha = 0$  and  $\alpha = \pi$ , respectively. Moreover, the wave-like amplitude in  $|\psi_{\mathbf{a}}\rangle$  is clearly related to the visibility  $\mathcal{V}$ . The scenario is such that by looking at the statistics at the output of the circuit, one infers the way the qubit travelled the interferometer. However, as natural this argument may sound, it suffers from an important flaw: regardless of how high  $\mathcal{V}$  may be, thus presuming an accentuated wave-like behaviour, the qubit state inside the interferometer invariably is  $|\varphi_\theta\rangle$ , which has been assumed to be linked with particle-like behaviour. If, on the other hand, we argue that this state cannot be used to account for the qubit route, then we are somehow conceiving that quantum mechanics is not complete. To further stress the issue, we compute realism inside the circuit. Let us define  $P \equiv \sigma_z$  and  $W \equiv \sigma_x$ , with respective eigenstates  $\{|\mathcal{P}_+\rangle, |\mathcal{P}_-\rangle\} \equiv \{|0\rangle, |1\rangle\}$  and  $|\mathcal{W}_\pm\rangle = \frac{1}{\sqrt{2}}(e^{i\theta}|0\rangle \pm |1\rangle)$ , as the relevant eigenstates for the particle and wave observables, respectively. This choice naturally connects definite paths,  $|\mathcal{P}_\pm\rangle$ , with particle-like elements of reality, that is,  $\Re_P(\mathcal{P}_\pm) = 1$  and  $\Re_W(\mathcal{P}_\pm) = 0$ . On the other hand, superposed paths imply wave-like elements of reality (wave reality, for short), that is,  $\Re_W(\mathcal{W}_\pm) = 1$  and  $\Re_P(\mathcal{W}_\pm) = 0$ . For  $|\varphi_\theta\rangle$ , direct calculations yield

$$\Re_P(|\varphi_\theta\rangle) = 0 \quad \text{and} \quad \Re_W(|\varphi_\theta\rangle) = 1, \quad (4)$$

showing that the so-called particle-like state actually corresponds to a wave reality. Therefore, in full contrast to current claims, inside the interferometer the qubit always behaves as a wave and  $\mathcal{V}$  does not faithfully furnish this diagnosis. It follows that the pattern  $\mathbf{p}_0$ , for  $0 < \alpha < \pi$ , cannot validate the manifestation of morphing behaviour in the setup of Fig. 1(a).

*Quantumly controlled reality experiment (QCRE).* We now propose an experiment that aims at solving the aforementioned issues and effectively superposing wave and particle elements of reality. Consider the setup depicted in Fig. 1(b), which implements a simple exchange in the devices order. The input state  $|\psi_{\text{in}}\rangle = |0\rangle(\cos\frac{\alpha}{2}|\text{in}\rangle + \sin\frac{\alpha}{2}|\text{out}\rangle)$  now results in  $|\psi_{\mathbf{b}}\rangle = \cos\frac{\alpha}{2}|w_\theta\rangle|\text{in}\rangle + e^{i\theta}\sin\frac{\alpha}{2}|\varphi_\pi\rangle|\text{out}\rangle$ , thus yielding precisely the same interference pattern  $\mathbf{p}_0 = \frac{1}{2}(1 + \mathcal{V}\cos\theta)$  and visibility  $\mathcal{V} = \cos^2(\frac{\alpha}{2})$ . Clearly, with respect to the

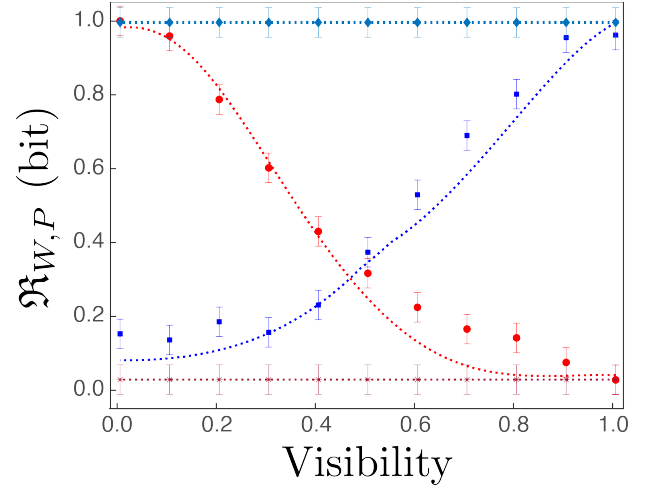


FIG. 2. Wave and Particle Realism as a function of the Visibility. The cyan diamonds and dark red stars are the measured  $\Re_W$  and  $\Re_P$ , respectively, inside of the interferometer with the arrangement in Fig. 1(a). The blue squares and red circles are the measured  $\Re_W$  and  $\Re_P$ , respectively, inside of the interferometer of Fig. 1(b). The symbols represent the experimental results and the dashed lines numerical simulations.

statistics observed at the output, nothing changes. However, the states inside the interferometer (right after the phase shifter) are

$$|\phi_{\text{QDCE}}\rangle = |\varphi_\theta\rangle(\cos\frac{\alpha}{2}|\text{in}\rangle + \sin\frac{\alpha}{2}|\text{out}\rangle), \quad (5a)$$

$$|\phi_{\text{QCRE}}\rangle = \cos\frac{\alpha}{2}|\mathcal{W}_+\rangle|\text{in}\rangle + e^{i\theta}\sin\frac{\alpha}{2}|\mathcal{P}_+\rangle|\text{out}\rangle, \quad (5b)$$

with  $|\varphi_\theta\rangle = \cos\theta|\mathcal{W}_+\rangle - i\sin\theta|\mathcal{W}_-\rangle$ . The differences are remarkable. Correlations are seen to play no role in the original setup, so that there is not an effective “whole” defining the behavior of the qubit at this stage. The interference device puts the qubit in a superposition of paths, which implies a wave reality:

$$\Re_W(\phi_{\text{QDCE}}) = 1, \quad \Re_P(\phi_{\text{QDCE}}) = 0. \quad (6)$$

In the new setup, when the controlled device is deactivated, the qubit just keeps travelling its original path, as a particle, this being a key difference to the QDCE. State (5b) predicts a clear superposition of two orthogonal reality scenarios: one wave-like ( $|\mathcal{W}_+\rangle|\text{in}\rangle$ ) and another particle-like ( $|\mathcal{P}_+\rangle|\text{out}\rangle$ ). In addition, via direct calculations one finds

$$\Re_W(\phi_{\text{QCRE}}) = 1 - h\left(\frac{1-\mathcal{V}}{2}\right), \quad \Re_P(\phi_{\text{QCRE}}) = 1 - h\left(\frac{\mathcal{V}}{2}\right), \quad (7)$$

where  $h(u) = -u\log_2 u - (1-u)\log_2(1-u)$  is the binary entropy. These relations show that  $\Re_W(\Re_P)$  is a monotonically increasing (decreasing) function of the visibility  $\mathcal{V}$ . Hence, in contrast to the QDCE, here we have a strict equivalence between the output statistics and the wave-like behavior inside the interferometer. Note that within

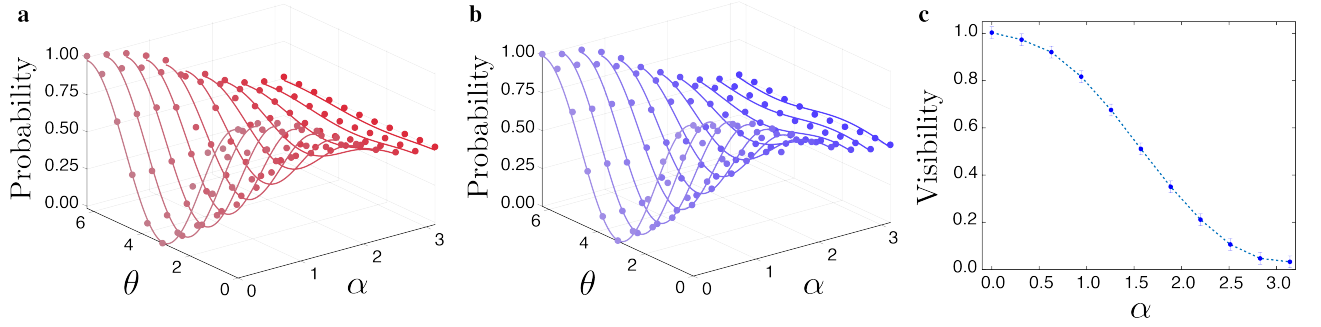


FIG. 3. Probability pattern at the end of the interferometer ( $\mathbf{p}_0$ ) as function of the interference parameter ( $\alpha$ ) and the phase sifter ( $\theta$ ). (a) For quantum controlled delayed choice scenario (setup in Fig. 1 (a)). (b) For quantum controlled realism scenario (setup in Fig. 1(b)). (c) Visibility ( $\mathcal{V}$ ) of the interferometer in the quantum controlled realism scenario. The symbols represent the experimental results and the (solid and dashed) lines numerical simulations.

the domain  $\alpha \in [0, \pi]$ , the visibility  $\mathcal{V}$  at the output and the wave and particle realisms  $\mathfrak{R}_{W,P}$  inside the interferometer are monotonic functions of  $\alpha$ , meaning that these quantities can be controlled by the preparation of the quantum controller  $\mathcal{C}$ . Also, relation (3) here reduces to

$$\mathfrak{R}_W(\phi_{\text{QCRE}}) + \mathfrak{R}_P(\phi_{\text{QCRE}}) \leq 1 - h\left(\frac{1 + \lambda_{\mathcal{V}}}{2}\right), \quad (8)$$

where  $\lambda_{\mathcal{V}} \equiv \sqrt{2\mathcal{V}^2 - 2\mathcal{V} + 1}$ . Interestingly, this result as a function of  $\mathcal{V}$  demonstrates how quantum correlations between the qubit and the quantum controller are sufficient to deny classical realism inside the interferometer to both complementary observables at the same time, thus corroborating Bohr's original formulation of the complementarity principle.

We implemented the above ideas in a proof-of-principle experiment using a liquid-state NMR setup with two spin-1/2 qubits encoded in a sample of  $^{13}\text{C}$ -labelled  $\text{CHCl}_3$  (Chloroform) diluted in Acetone- $d_6$ . The experiments were carried out in a Varian 500 MHz spectrometer. The  $^{13}\text{C}$  nuclear spin was used as the ancillary control of the interferometric device to investigate the realism, wave and particle features of the  $^1\text{H}$  nuclear spin (which encompass the interferometric paths). The nuclear spins were initially prepared in a state equivalent to  $\rho = |\psi_{\text{in}}\rangle\langle\psi_{\text{in}}|$ , using spatial averages techniques [40] (see the Appendix).

All the spin-1/2 quantum controlled interferometric protocols in Fig. 1(a)(b) were performed using combinations of transverse radio-frequency pulses on resonance with each nuclei and sequences of free evolution under the spin scalar coupling,  $H_J = J_4^h \sigma_Z^H \otimes \sigma_Z^C$ , with  $\sigma_Z^{H(C)}$  being the Pauli operator for the  $^1\text{H}$  ( $^{13}\text{C}$ ) nuclear spin and  $J \approx 215.1$  Hz the coupling constant. The realism (displayed in Fig. 2) is quantified performing full quantum state tomography [40] along the interferometric protocol

with different values of the interference control parameter  $\alpha$  and the phase sifter  $\theta$  for each setup in Fig. 1 (a)(b). The interferometric pattern ( $\mathbf{p}_0$ ) is observed directly from the  $^1\text{H}$  nuclear spin magnetization in the  $z$ -direction at the end of the protocols.

Wave and particle are classical physics terms employed for one to discuss the behaviour of a quantum system that traverses a double-path setup and produces some signals and statistics in the output measurement device. When the signal pattern depends on the difference of phases between the paths, the behavior is claimed to be wave-like. However, in the QDCE the output visibility does not tell an unambiguous story about the qubit behaviour inside the circuit. The state inside the interferometer—the so-called particle state,  $|\wp_\theta\rangle$ —has spatial coherences, a resource that can be used to create entanglement between distinct quantum systems [21]. It is hard to imagine that a presumably well-localized system (a particle), developing a (hidden) realistic trajectory in space-time, be able to touch space-like separated systems. The strategy of making inferences about past behaviour (inside the circuit) with basis on present observations (at the output) diminishes the significance of the quantum state and favours the view according to which quantum mechanics is not a complete theory. In addition, the statistics-based criterion does not shed light on another challenging aspect of typical double-path experiments: even when the observed pattern is wavelike, in each run of the experiment only one of the detectors is activated (this point is discussed in detail in the Appendix.)

The realism-based framework we developed here makes a rather different narrative for the QDCE and introduces a QCRE, an arrangement that has the same output visibility of the former, as demonstrated in Fig. 3(a)(b), but whereby Bohr's original formulation of the complementarity principle can be afforded, as we show next,



a deeper and broader significance. As theoretically predicted [Eq. (6)] and experimentally corroborated (Fig. 2 and Fig. 3(a)(b)(c)), wave and particle elements of reality inside the circuit are fully disconnected from the output visibility, so that no wave-particle superposition or morphing behavior can actually be claimed in the QDCE. The scenario is quite the opposite in the QCRE, where wave and particle elements of reality are regulated by the initial coherence of the quantum controller and turn out to be monotonically linked with the visibility, as demonstrated by Eq. (7) and Fig. 2. Equation (5b) and our experimental demonstration arguably show, for the first time (to the best of our knowledge), the possibility of genuinely superposing wave and particle elements of reality to an arbitrary degree. By employing the figures of merit  $\mathfrak{R}_{W,P}(\rho)$ , which lies solely on the time-local context defined by the composite state  $\rho$  and observables  $\{W, P\}$ , thus respecting premises of standard quantum mechanics, our model avoids retro-causal inferences and suitably describe “the whole”.

Most interestingly, the QCRE allows for the manifestation of “morphing realities” (for  $0 < \mathcal{V} < 1$ ), the inequality (8) prevents  $W$  and  $P$  to be simultaneous elements of reality. In fact, referring back to the general scenario underlying inequality (3), one can check that the upper bound can be written as  $2 \log_2 d_A - S\left(\rho \parallel \frac{1}{d_A} \otimes \rho_B\right)$ . This demonstrates that  $\rho = \frac{1}{d_A} \otimes \rho_B$  is the only state admitting the saturation  $\mathfrak{R}_A = \mathfrak{R}_{A'} = \log_2 d_A$ , for all  $A$  and  $A'$ , in which case full realism emerges in the part  $\mathcal{A}$  (classical regime). For any other (non-classical) state, the mutual exclusiveness of realism is implied. To further appreciate this point, it is instructive to use the conditional entropy  $S_{A|B}(\rho) = S(\rho) - S(\rho_B)$  and the conditional information  $I_{A|B}(\rho) = \log_2 d_A - S_{A|B}(\rho)$  to rewrite inequality (3) in the form

$$\mathfrak{R}_A(\rho) + \mathfrak{R}_{A'}(\rho) \leq 2 \log_2 d_A - I_{A|B}(\rho). \quad (9)$$

Also, it is noteworthy that  $I_{A|B}(\rho) = I(\rho_A) + I_{A:B}(\rho)$ , with  $I(\rho_A) = \log_2 d_A - S(\rho_A)$  being a purity measure for the reduced state. These relations help us to make a fundamental point: *the purity of a system and the correlations shared with “the whole” prevent it to have simultaneous elements of reality.* In other words, provided we consider a quantum state for a composite system (“the whole”) in a given setting, even in a quantumly controlled one, wave and particle realities can never manifest themselves simultaneously. Such statements stand out in full opposition to the Einstein, Podolsky, and Rosen (EPR) arguments about physical reality [41] and validate Bohr’s philosophy. Finally, we highlight that our work sheds light on the role of the complementarity principle in the context of morphing reality states submitted to a quantum controlled operation, which may lead to new insights regarding the nature of quantum causality, quantum reference frames, and, specially, a renewal of the discussion

on the realistic aspects of wave and particle properties linked to quantum systems.

## ACKNOWLEDGMENTS

The authors acknowledge the Brazilian funding agencies Coordenação de Aperfeiçoamento de Pessoal de Nível Superior-Brasil (CAPES)–Finance Code 001 (grant 88887.354951/2019-00, P.R.D), FAPESP, CNPq (grant 309373/2020-4, R.M.A.), and the National Institute for Science and Technology of Quantum Information (CNPq, INCT-IQ 465469/2014-0). The authors are grateful to the Multiuser Central Facilities (UFABC) for the experimental support. J.P.S.P. thanks support from Innovation, Science and Economic Development Canada, the Government of Ontario, and CIFAR.

- 
- [1] N. Bohr, Can quantum-mechanical description of physical reality be considered complete?, *Phys. Rev.* **48**, 696 (1935).
  - [2] S. Saunders, Complementarity and Scientific Rationality, *Found. Phys.* **35**, 417 (2005).
  - [3] J. A. Wheeler in *Quantum Theory and Measurement*, 182-213, eds J. A. Wheeler and W. H. Zurek (Princeton University Press, 1983).
  - [4] V. Jacques, E Wu, F. Grosshans, F. Treussart, P. Grangier, A. Aspect, and J-F. Roch, Experimental realization of Wheeler’s delayed-choice gedanken experiment, *Science* **315**, 966-968 (2007).
  - [5] A. G. Manning, R. I. Khakimov, R. G. Dall, A. G. Truscott, Wheeler’s delayed-choice gedanken experiment with a single atom, *Nat. Phys.* **11**, 539–542 (2015).
  - [6] F. Vedovato, C. Agnesi, M. Schiavon, D. Dequal, L. Calderaro, M. Tomasin, D. G. Marangon, A. Stanco, V. Luceri, G. Bianco, G. Vallone, P. Villoresi, Extending Wheeler’s delayed-choice experiment to space, *Sci Adv* **3**, e1701180 (2017).
  - [7] A. Peres, Delayed choice for entanglement swapping, *J. Mod. Opt.* **47**, 139–143 (2000).
  - [8] T. Jennewein, M. Aspelmeyer, Č. Brukner, A. Zeilinger, Experimental proposal of switched delayed-choice for entanglement swapping, *Int. J. Quant. Info.* **3**, 73-79 (2005).
  - [9] Č. Brukner, M. Aspelmeyer, A. Zeilinger, Complementarity and information in “delayed-choice for entanglement swapping”, *Found. of Phys.* **35**, 1909–1919 (2005).
  - [10] F. Sciarrino, E. Lombardi, G. Milani, F. De Martini, Delayed-choice entanglement swapping with vacuum–one-photon quantum states, *Phys. Rev. A* **66**, 024309 (2002).
  - [11] X-s. Ma, S. Zotter, J. Kofler, R. Ursin, T. Jennewein, Č. Brukner, A. Zeilinger, Experimental delayed-choice entanglement swapping, *Nat. Phys.* **8**, 479–484 (2012).
  - [12] R. Ionicioiu and D. R. Terno, Proposal for a Quantum Delayed-Choice Experiment, *Phys. Rev. Lett.* **107**, 230406 (2011).
  - [13] R. Auccaise, R. M. Serra, J. G. Filgueiras, R. S. Sarthour, I. S. Oliveira, L. C. Céleri, Experimental analysis of the

- quantum complementarity principle, *Phys. Rev. A* **85**, 032121 (2012).
- [14] S. S. Roy, A. Shukla, and T. S. Mahesh, NMR implementation of a quantum delayed-choice experiment, *Phys. Rev. A* **85**, 022109 (2012).
- [15] A. Peruzzo, P. Shadbolt, N. Brunner, S. Popescu, J. L. O'Brien, A Quantum Delayed-Choice Experiment, *Science* **338**, 634-637 (2012).
- [16] F. Kaiser, T. Coudreau, P. Milman, D. B. Ostrowsky, S. Tanzilli, Entanglement-Enabled Delayed-Choice Experiment, *Science* **338**, 637-640 (2012).
- [17] G. Adesso and D. Girolami, Wave-particle superposition, *Nat. Photonics* **6**, 579 (2012).
- [18] A. S. Rab, E. Polino, Z.-X. Man, N. B. An, Y.-J. Xia, N. Spagnolo, R. L. Franco, and F. Sciarrino, Entanglement of photons in their dual wave-particle nature, *Nat. Commun.* **8**, 915 (2017).
- [19] K. Liu, Y. Xu, W. Wang, S.-B. Zheng, T. Roy, S. Kundu, M. Chand, A. Ranadive, R. Vijay, Y. Song, L. Duan, L. Sun, A twofold quantum delayed-choice experiment in a superconducting circuit, *Sci. Adv.* **3**, e1603159 (2017).
- [20] K. Wang, Q. Xu, S. Zhu, and X.-S. Ma, Quantum wave-particle superposition in a delayed-choice experiment, *Nat. Photonics* **13**, 872 (2019).
- [21] R. M. Angelo and A. D. Ribeiro, Wave-particle duality: an information-based approach, *Found. Phys.* **45**, 1407 (2015).
- [22] P. J. Coles, J. Kaniewski, and S. Wehner, Equivalence of wave-particle duality to entropic uncertainty, *Nat. Commun.* **5**, 5814 (2014).
- [23] R. Chaves, G. B. Lemos, and J. Pienaar, Causal Modeling the Delayed-Choice Experiment, *Phys. Rev. Lett.* **120**, 190401 (2018).
- [24] A. L. O. Bilobran and R. M. Angelo, A measure of physical reality, *Europhys. Lett.* **112**, 40005 (2015).
- [25] P. R. Dieguez, R. M. Angelo, Information-reality complementarity, The role of measurements and quantum reference frames, *Phys. Rev. A* **97**, 022107 (2018).
- [26] V. S. Gomes, R. M. Angelo, Nonanomalous realism-based measure of nonlocality, *Phys. Rev. A* **97**, 012123 (2018).
- [27] V. S. Gomes, R. M. Angelo, Resilience of realism-based nonlocality to local disturbance, *Phys. Rev. A* **99**, 012109 (2019).
- [28] D. M. Fucci and R. M. Angelo, Tripartite realism-based quantum nonlocality, *Phys. Rev. A* **100**, 062101 (2019).
- [29] L. Rudnicki, Uncertainty-reality complementarity and entropic uncertainty relations, *J. Phys. A* **51**, 504001 (2018).
- [30] A. C. Orthey Jr. and R. M. Angelo, Nonlocality, quantum correlations, and violations of classical realism in the dynamics of two noninteracting quantum walkers, *Phys. Rev. A* **100**, 04110 (2019).
- [31] N. G. Engelbert and R. M. Angelo, Hardy's paradox as a demonstration of quantum irrealism, *Found. Phys.* **50**, 105 (2020).
- [32] F. R. Lustosa, P. R. Dieguez, and I. G. da Paz, Irrealism from fringe visibility in matter-wave double-slit interference with initial contractive states, *Phys. Rev. A* **102**, 052205 (2020).
- [33] L. Mancino, M. Sbroscia, E. Roccia, I. Gianani, V. Cimini, M. Paternostro, and M. Barbieri, Information-reality complementarity in photonic weak measurements, *Phys. Rev. A* **97**, 062108 (2018).
- [34] A. C. S. Costa and R. M. Angelo, Information-based approach towards a unified resource theory, *Quantum Info. Process.* **19**, 325 (2020).
- [35] H. Ollivier and W. H. Zurek, Quantum discord: A measure of the quantumness of correlations, *Phys. Rev. Lett.* **88**, 017901 (2001).
- [36] L. Henderson and V. Vedral, Classical, quantum and total correlations, *J. Phys. A: Math. Gen.* **34**, 6899 (2001); V. Vedral, Classical correlations and entanglement in quantum measurements, *Phys. Rev. Lett.* **90**, 050401 (2003).
- [37] L. C. Céleri, J. Maziero, and R. M. Serra, Theoretical and experimental aspects of quantum discord and related measures, *Int. J. Quantum Inform.* **9**, 1837 (2011).
- [38] K. Modi, A. Brodutch, H. Cable, T. Paterek, and V. Vedral, The classical-quantum boundary for correlations: Discord and related measures, *Rev. Mod. Phys.* **84**, 1655 (2012).
- [39] I. S. Freire and R. M. Angelo, Quantifying continuous-variable realism, *Phys. Rev. A* **100**, 022105 (2019).
- [40] I. S. Oliveira, T. J. Bonagamba, R. S. Sarthour, J. C. C. Freitas, R. R. deAzevedo, *NMR Quantum Information Processing* (Elsevier, Amsterdam, 2007).
- [41] A. Einstein, B. Podolsky, and N. Rosen, Can quantum-mechanical description of physical reality be considered complete?, *Phys. Rev.* **47**, 777 (1935).
- [42] T. B. Batalhão, A. M. Souza, L. Mazzola, R. Auccaise, R. S. Sarthour, I. S. Oliveira, J. Goold, G. De Chiara, M. Paternostro, and R. M. Serra, Experimental reconstruction of work distribution and study of fluctuation relations in a closed quantum system, *Phys. Rev. Lett.* **113**, 140601 (2014).
- [43] T. B. Batalhão, A. M. Souza, R. S. Sarthour, I. S. Oliveira, M. Paternostro, E. Lutz, and R. M. Serra, Irreversibility and the arrow of time in a quenched quantum system, *Phys. Rev. Lett.* **115**, 190601 (2015).
- [44] E. Knill, I. Chuang, and R. Laflamme, Effective pure states for bulk quantum computation, *Phys. Rev. A*, **57**, 3348 (1998).

## I. APPENDIX

### 1. Experimental Setup

In the reported experiments we used a liquid sample of  $^{13}\text{C}$ -labelled  $\text{CHCl}_3$  (Chloroform) diluted in Acetone- $d_6$ , the Chloroform molecules in the sample were composed of four nuclei (isotopes):  $^1\text{H}$ ,  $^{13}\text{C}$ ,  $^{35}\text{Cl}$ , and  $^{37}\text{Cl}$ . We only controlled the  $^1\text{H}$  and  $^{13}\text{C}$  nuclei. As a consequence of the preparation, the sample is very diluted in Acetone- $d_6$ , such that the Chloroform inter-molecular interactions can be neglected and the sample is considered as a set of identically prepared pairs of spin-1/2 systems (multiple copies of a two-qubit system). The Chlorine only provides mild environmental effects in the experiments.

The experiments were performed using a Varian 500 MHz spectrometer equipped with a superconducting magnet, double-resonance probe head with magnetic field-gradient coil. The magnetometer produces a static field with  $B_0 \approx 11.75$  T of intensity, along the positive z-axes (parallel to the central axis of the superconducting magnet). Under the action of this static field, the resonance frequencies of  $^1\text{H}$  and  $^{13}\text{C}$  are approximately 500 MHz and 125 MHz, respectively. The state of the nuclear spins are controlled by time-modulated radio frequencies pulses (rf-pulses) in the transverse direction (x and y), longitudinal field gradients, as well as by sequences of free evolution of the system under the action of scalar coupling interactions. The latter is described by the Hamiltonian  $H_J = J \frac{\hbar}{4} \sigma_Z^H \otimes \sigma_Z^C$ , where  $J \approx 215.1$  Hz is the coupling constant between the  $^1\text{H}$  and  $^{13}\text{C}$  nuclear spins.

Measured by inversion recovery, the spin-lattice relaxation times were found to be  $T_1^H = 8.882$  s and  $T_1^C = 18.370$  s. In the case of transverse relaxations, the characteristics times were obtained by the Carr-Purcell-Meiboom-Gill (CPMG) pulse sequence, resulting in  $T_2^H = 2.185$  s and  $T_2^C = 0.310$  s. The interferometric protocols in the experiments were performed in a time scale of  $\approx 14$  ms, which is sufficiently smaller than the aforementioned decoherence times for neglecting its effects.

The effective initial state of the nuclear spins were prepared by spatial average techniques [40, 42, 43], being the  $^1\text{H}$  and  $^{13}\text{C}$  nuclei used as the system of interest and ancillary control, respectively. For both cases shown in Fig. 1(a)(b) of the main text, the initial pseudo-pure state [40, 44] equivalent to  $\rho = |\psi_{in}\rangle\langle\psi_{in}|$  was prepared by the pulse sequence depicted in Fig. 4.

In the building process of the quantum circuits implemented here, we constructed a sequence in order to make optimizations that are often needed to minimize the number of the experimental process and to improve the accuracy of the results. As discussed in the main text, each interferometer has a different protocol of implementation, corresponding to the original formulation QDCE, and our proposal of the quantum controlled real-

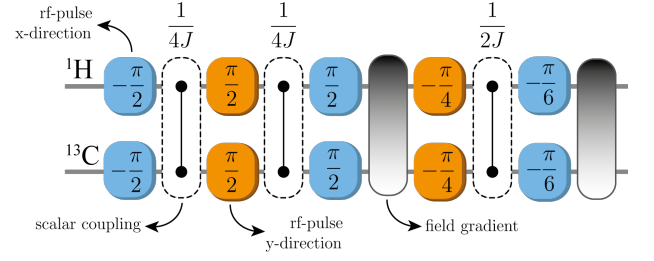


FIG. 4. Pulse sequence for the initial state preparation. The blue (orange) boxes represent x (y) local rotations by the angles indicated internally. These rotations are produced by a transverse rf-field resonant with either  $^1\text{H}$  or  $^{13}\text{C}$  nuclei, with phase, amplitude, and time duration suitably adjusted. The dashed boxes with connections represent free time evolutions. The boxes with gradient color represent magnetic field gradients, with longitudinal orientations aligned with the spectrometer cylindrical symmetry axis. All the control parameters are optimized to build an initial pseudo-pure state equivalent to  $\rho = |00\rangle\langle 00|$  with high fidelity ( $\gtrsim 0.99$ ).

ity scenario (QCRE). The correspondent pulse sequences to each scenario are presented in Fig. 5(a)(b).

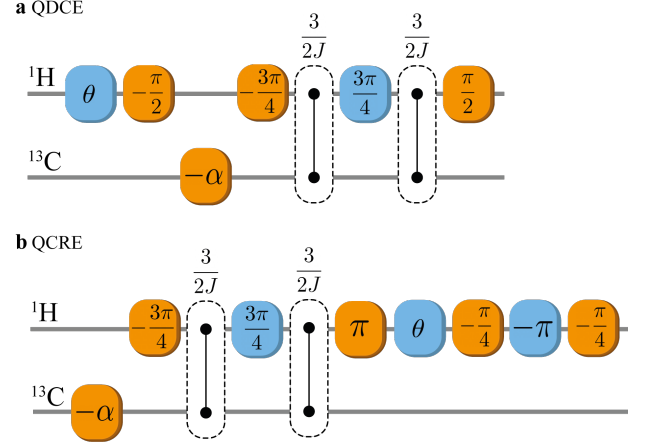


FIG. 5. Pulse sequences for the two interferometer scenarios. (a) Original version of the QDCE scenario. For the sake of optimization, the first superposition device and the phase shifter were implemented by two operations ( $\theta$  and  $-\frac{\pi}{2}$ ). The quantum controlled interference was performed using local operations on the main system and on the controller, as well as free evolutions involving both qubits (beginning at the  $-\alpha$  rotation). (b) For the QCRE scenario, the quantum controlled interference has a similar structure (starting at the  $-\alpha$  rotation and ending at  $\pi$ ), the only difference is the last rotation. The phase shifter and the superposition device were implemented with four operations (from the  $\theta$  rotation to  $-\frac{\pi}{4}$ ). Although the QCRE seems to last longer, the most relevant contributions to the total duration of each experiment were the free evolutions, and that is the reason why both experiments last approximately the same period ( $\approx 14$  ms).

## 2. Error Analysis

The main source of experimental error are small uncontrolled variations on the transverse rf-fields, non-idealities in its time modulation and inhomogeneities in the longitudinal static field as well as in the gradient pulses. The process to estimate the error propagation is based on a Monte Carlo method, sampling deviations of the quantum state tomography (QST) data with a Gaussian distribution having widths determined by the variances corresponding to such data. These data give us the necessary information to estimate the standard deviation of the distribution of values for relevant quantities displayed in the figures. The variances of the tomographic data are obtained by preparing the same state one hundred times, taking the full state tomography and comparing it with the theoretical expectation. Such procedure makes these variances include random and systematic errors in both state preparation and data acquisition by QST. The error in each element of the density matrix estimated from this analysis is about 1%. The majority of the experimental parameters, such as pulses intensity, phase, time duration, gradient variation, free evolution interval, and field's homogeneity are optimized in order to minimize errors.

## 3. Realism and the measurement problem

Electing the relation (9) as a formal statement of Bohr's complementarity principle also proves insightful with respect to the measurement problem, which here can be linked with the individual data acquisition in each run of the experiment. For illustration, let us consider only the open configuration of the QDCE. Let us take  $|\mathbf{r}_k\rangle$  ( $\mathbf{r} \equiv$  ready) and  $|\mathbf{a}_k\rangle$  ( $\mathbf{a} \equiv$  activated) as orthogonal internal states of the  $k$ -th detector. Here we take the perspective of the von-Neumann measurement model, which

includes the measurement apparatus as a piece of “the whole”. After the entire dynamics takes place, the state of the joint system becomes

$$|\Psi_{\mathbf{a}}\rangle = |\text{out}\rangle \left( \frac{|0\rangle|\mathbf{a}_0\rangle|\mathbf{r}_1\rangle + e^{i\theta}|1\rangle|\mathbf{r}_0\rangle|\mathbf{a}_1\rangle}{\sqrt{2}} \right). \quad (10)$$

Now comes the crux: as recognised in Ref. [25], in all measurement processes the physical quantity to be observed is never directly accessed and actually is discarded. In fact, we read a degree of freedom of the apparatus, which has got correlated with the desired quantity. For instance, in the Stern-Gerlach setup, we read the position of the particle (“the apparatus”) to get to know about the spin (the discarded degree of freedom). In the present instance, we can trace the qubit path out of the state (10), since this degree of freedom is never effectively accessed in the experiment. This gives

$$\varsigma = \frac{|\text{out}\rangle\langle\text{out}|}{2} \otimes \left( |\mathbf{a}_0\rangle\langle\mathbf{a}_0| \otimes |\mathbf{r}_1\rangle\langle\mathbf{r}_1| + |\mathbf{r}_0\rangle\langle\mathbf{r}_0| \otimes |\mathbf{a}_1\rangle\langle\mathbf{a}_1| \right). \quad (11)$$

If we adopt  $|\mathcal{P}_k^+\rangle \equiv |\mathbf{a}_k\rangle$  and  $|\mathcal{P}_k^-\rangle \equiv |\mathbf{r}_k\rangle$  as particle-like states for the  $k$ -th detector (expressing definiteness of the detector internal state) and  $|\mathcal{W}_k^\pm\rangle \equiv (|\mathbf{a}_k\rangle \pm |\mathbf{r}_k\rangle)/\sqrt{2}$  as wave-like states, then we can show that

$$\Re_{P_k}(\varsigma) = 1 \quad \text{and} \quad \Re_{W_k}(\varsigma) = 0, \quad (12)$$

meaning that the internal states of the detectors, for the accessible context, are elements of reality. Therefore, unlike the statistic-base criterion, our model is able to explain why we do not find the detection system in a superposition of realities  $|\mathbf{a}_0\rangle|\mathbf{r}_1\rangle$  and  $|\mathbf{r}_0\rangle|\mathbf{a}_1\rangle$ .